

See discussions, stats, and author profiles for this publication at: <https://www.researchgate.net/publication/352536172>

# Low-cost 3D LIDAR-based scanning system for small objects

Conference Paper · March 2021

DOI: 10.1109/ICIT46573.2021.9453657

CITATIONS

5

READS

871

4 authors:



**João Braun**

Instituto Politécnico de Bragança

21 PUBLICATIONS 37 CITATIONS

[SEE PROFILE](#)



**José Lima**

Instituto Politécnico de Bragança

213 PUBLICATIONS 1,021 CITATIONS

[SEE PROFILE](#)



**Ana I. Pereira**

Instituto Politécnico de Bragança

166 PUBLICATIONS 536 CITATIONS

[SEE PROFILE](#)



**Paulo José Cerqueira Gomes da Costa**

University of Porto

224 PUBLICATIONS 1,233 CITATIONS

[SEE PROFILE](#)

Some of the authors of this publication are also working on these related projects:



Agriculture and Forest Robotics [View project](#)



Autonomous Legged-Wheeled Robotic Platform [View project](#)

# Low-cost 3D LIDAR-based scanning system for small objects

João A. Braun Neto

*Research Centre of Digitalization and Intelligent Robotics  
Instituto Politécnico de Bragança  
Mountains of Research Collaborative Laboratory  
Faculty of Engineering of University of Porto  
0000-0003-0276-4314*

Ana Isabel Pereira

*Research Centre of Digitalization and Intelligent Robotics  
Instituto Politécnico de Bragança  
Algoritmi of University of Minho  
0000-0003-3803-2043*

José Luís Lima

*Research Centre of Digitalization and Intelligent Robotics  
Instituto Politécnico de Bragança  
Bragança, Portugal  
INESC Technology and Science  
0000-0001-7902-1207*

Paulo Costa

*Faculty of Engineering of University of Porto  
Porto, Portugal  
INESC Technology and Science  
0000-0002-4846-271X*

**Abstract**—Three-dimensional scanning is a task that is highly important for our modern society and this is translated by a wide area of knowledge that contains numerous approaches to this task. As this process is non-trivial, most of the technologies are expensive, with even the low-cost ones being a great investment for the regular user. Therefore, this work presents a low-cost LIDAR-based 3D scanning system that can perform 3D scans of small objects and reconstruct their digital STL models. The system consists of one rotating platform and a scanning arc-shaped structure, which both are actuated by stepper motors.

**Index Terms**—3D scanning, LIDAR, digital reconstruction, Simulation, STL

## I. INTRODUCTION

Three-dimensional scanning of real-life objects is an important task for many areas of society as it allows for interaction with the digitized replica by software. According to [1], it makes it possible to generate new objects by 3D printing, facilitates reverse engineering and replication of artifacts without risking damaging cultural heirlooms. Also, the image can be used to create holograms and support applications that require human body imaging. Moreover, it is possible to scan objects such as the human body to create animations or support virtual reality applications [5].

As stated by [2], there are several approaches to 3D scanning, including laser and imagery based scanning techniques. Laser-based systems are abundant but expensive. Imagery-based systems, on the other hand, are available between low-cost, generally low-quality, and expensive higher-quality modules. One such example for expensive high-quality scanning system is cited by [5], where for Cultural Heritage projects the scanning system can cost more than 100K US\$.

This paper presents a simulated low-cost 3D scanning system with a reconstruction algorithm. This system uses a low-cost LIDAR (Light Detecting and Ranging) device to scan a point cloud from the object. Afterward, the point cloud is

processed by a reconstruction algorithm that generates the STL file.

A brief state of the art is described in Section II. Section III describes the 3D scanning system, how it works, and the reconstruction algorithm. The results are described in Section IV. Finally, the conclusion and future works are stated in Section V.

## II. STATE OF ART

As briefly mentioned in I, 3D scanning has a diverse spectrum of applications with a wide object scale size. This chapter will provide some recent related works in this area of knowledge. For a complete survey on the area, the reader is referred to [4], [9]. As previously mentioned in Section I, this work uses a LIDAR laser rangefinder. This device basically works by emitting a laser pulse to the object, and the distance between the transmitter and the reflecting surface is computed by the travel time from the transmission and the reception [13]. These sensors use small rotating mirrors to scan an angular range, measuring the distance at specific angle intervals. There is ongoing research to develop more efficient and low-cost measurement instruments, such as low-cost LIDARs. Authors in [11], developed a small, low-cost, and light weight LIDAR. Their device can obtain a 3D range data of 8000 points in 20 Hz with 270 degrees horizontal and 40 degrees vertical views in indoor and outdoor environments.

A large and low-cost instant 3D scanner was developed by [1] at the University of North Dakota to create 3D models for printing and other uses. According to the author, the budget was about 3500 US\$ and most of it was spent on 50 Raspberry Pi's and cameras. The digital Michelangelo Project is presented in [6], where it describes the hardware and software system for digitizing the shape and color of fragile objects. According to the authors, the system has laser triangulation rangefinders, laser time of flight rangefinders, digital still

cameras, and software programs to process the data. It is also stated that their largest dataset contains 2 billion polygons and 7000 color images from the figure of David. Moreover, three-dimensional scanning systems with laser time-of-flight measurement devices are compared for their usability in different situations in [7]. The authors contribute with new methods that allow fast scanning. In addition, a fast 3D motion scanning with automatic compensation is presented in [8]. Their system utilizes stereo and active illumination based on phase-shift for robust and accurate scene reconstruction. Also, a low-cost LIDAR-based system was developed in [10] to assess the feasibility of the inexpensive LIDAR sensor in leaf trait extraction. Furthermore, a 3D scanning system for deformable objects that utilizes only a Kinect sensor is described in [12]. Their system permits a good amount of nonrigid deformations during the scanning process and achieves high-quality results without restricting too much the user or camera motion.

### III. METHODOLOGY

The simulation environment used is the SimTwo simulator, a realistic simulator that uses rigid-body dynamics and simulates non-idealities and dynamic constraints from the real-world. For more information about the functionality of Simtwo, such as its features and how it works, please refer to [14]. The 3D scanning system is composed of a rotating platform, where the object will be scanned, and the scanning structure. The rotating platform is actuated by a stepper motor with a simple PID control. It is important to note that not only the real-world dynamics are simulated, but noise is also present. Finally, the scanned objects are described using the XML defined by the SimTwo simulator in its scene editor. The object description includes, but is not limited to: color, centroid pose, mass, size, type, centroid orientation, among others. Left illustration from Figure 1 illustrates the simulated scanning system.

The simulated world's reference system is indicated by the green arrows on the floor. The  $x$  axis is located in the right under the corner of the figure. The  $y$  axis is displayed in the upper right corner. The  $z$  axis is invisible for display purposes but can be computed using the right-hand rule. In addition, the scanning structure is invisible for simplicity reasons. The gray cylinder represents the LIDAR device, displayed by the orange arrow. The grey cube at the bottom represents the rotating platform, represented by the white arrow. Finally, the polyhedrons and the sphere on top of the platform are the objects to be scanned, represented by the cyan arrow.

The scanning system works basically in two steps. First, the object is scanned and a point cloud file is generated. Afterward, this file is read by a software program that was developed to reconstruct the digital object model. The first step is explained with more details below.

#### A. Laser scan

When the scanning process begins, the platform starts rotating in a known constant angular speed. At the same time, during each platform revolution, the LIDAR device scans the object in the plate at a certain angle in the arc-shaped structure.

After each revolution from the platform, the scanning structure performs increments in the arc's angle, that is, in relation to the  $XY$  plan. This way, during each revolution the device will scan new information until it reaches  $90^\circ$ . In this sense, the angular speed from the platform, the increment size in the scanning structure, and LIDAR operating frequency are ways to regulate scanning resolution.

As LIDAR returns the distance between the obstacle and the emitter, it is crucial to know the distance between the center of the rotating plate and the scanning device. Moreover, it is important to note that the rotating speed mustn't be too high because the objects can slip, affecting the device scan, thus the digital object reconstruction.

The scanning operation generates a text point cloud file that contains information about the 3D Cartesian coordinates of each point in relation to the rotating platform reference frame. Figure 2 displays an example of a point cloud file generated from a scanned cube object.

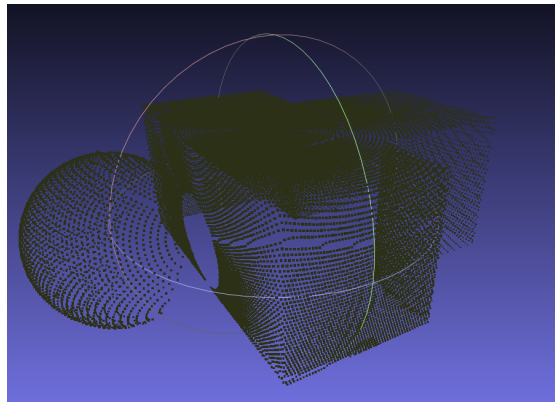


Fig. 2: Point cloud of the scanned object. Visualized in MeshLab.

The angular speed of the rotating plate affects the resolution, as can be clearly seen on the sphere's parts that are obscured by the bigger cube. Nevertheless, even with the noise and uncertainty of the LIDAR device (modeled in Simtwo), the point cloud shows a great resemblance of the "real-world" object. It is expected, as this point cloud has 32402 vertices. It was used the open-source MeshLab software to visualize the data.

During the scanning procedures, the points are gathered using cylindrical coordinates, as its advantageous trigonometry-wise, given the system's structure. Therefore, the total distance between the LIDAR transmitter and the center of the rotating plate is always the same, as the radius of a circumference arc is equidistant. Right illustration from Figure 1 illustrates the scanning system from a side view.

The distance obtained by the LIDAR device is represented by the dark red line. Thus, the  $XY$  plane projected difference between the total distance and the distance obtained by the current scan is  $\rho$ , which is represented by the light red line in the right illustration from Figure 1. The projection is computed using angle  $\phi$ , represented in the illustration. The angle of

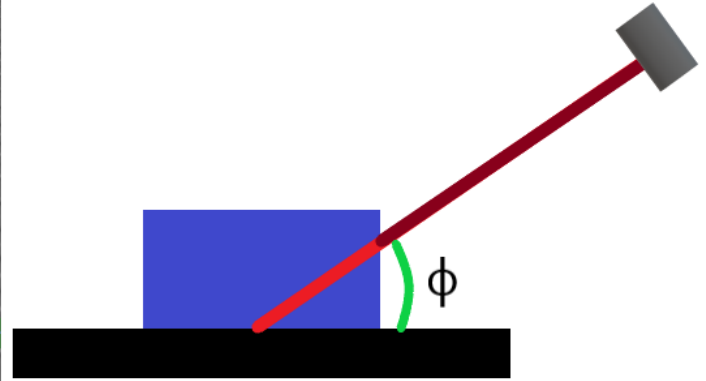
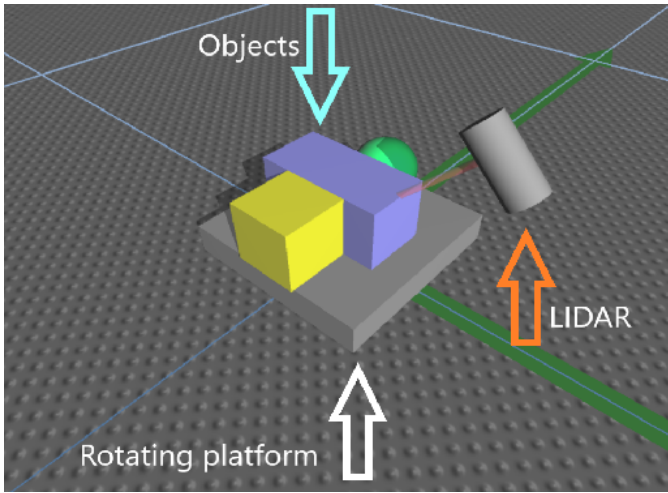


Fig. 1: Left figure: Simulated 3D scanning system in Simtwo simulator. Right figure: Side view illustration of the 3D scanning system.

the rotating plate is  $\theta$ , which is omitted from the figure, as it is a side view. Finally, with  $\phi$ ,  $Z$  is computed. After this, with simple trigonometry, it is possible to compute the transformation to the 3D Cartesian's coordinate system from the cylindrical system in relation to the platform's reference coordinate frame.

### B. Object reconstruction

The reconstruction algorithm generates the meshes taking into consideration the way the scan was done, i.e.,  $n$  columns of points from lowest to the highest angle of  $\phi$ . With this in mind, the meshes are built taking two adjacent columns per iteration. Specifically, two meshes are built for every four points of the adjacent columns, two points for each column. In other words, in the same way, a square can be divided in two triangles, two triangles are built with four points for every two adjacent columns. Therefore, the normal vectors are computed by cross-products to generate the orientation information for each triangle, and afterward, they are stored in an STL file.

This process will generate the meshes for the vast majority of the object. However, the bottom layer and a tiny space of the top layer of the object will not be generated. The reason this happens for the bottom layer is straightforward, as the scanning system assumes that the scanned object has a flat bottom layer, needing only two degrees of freedom to operate ( $\phi$  and  $\theta$ ). However, Figure 3 displays the top behaviour.

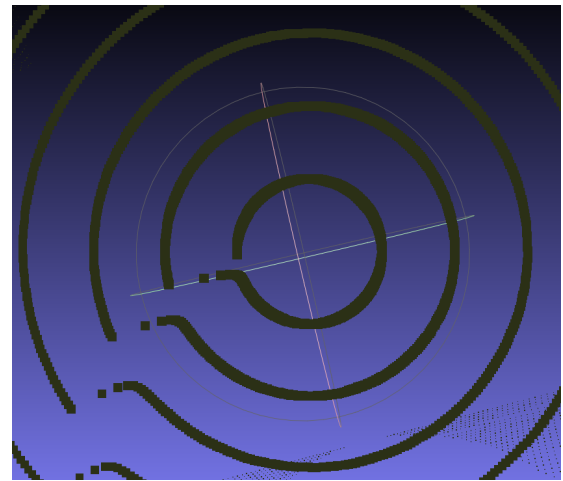


Fig. 3: Top layer of the scanned object. Visualized in MeshLab.

As can be noticed, the top layer is not computed because of the limitations of the system's structure. It doesn't matter the size of the resolution, always a tiny circle will be left out. Thus, the bottom layer and the top layer meshes are computed by averaging the position of all the points of the current  $Z$  and then creating the meshes with one vertex of the triangle being the averaged point, i.e., the center of the "open" space. Another behaviour that can be noted, is the discontinuities between each step from the scanning structure. This happens because the rotating plate does not stop for each step increment. To address this, the rotating plate would need to be synchronized with the scanning structure and stop the rotation at each increment.

As this system works with small objects and the resolution is very high, this simple solution is acceptable. After the computations, all the meshes are stored up in two STL files, one with the ASCII format for visibility purposes and the other with the binary format.

#### IV. RESULTS

It was scanned three arbitrary objects with a resolution of 1 degree in the scanning step size. The rotating platform was configured to rotate at an angular speed of 25 deg/s.

For the first example, the scan procedure took approximately 21 minutes and the STL generation procedure took approximately 2.4 seconds. The scan procedure takes a lot of time because the resolution is high. If the resolution was 5 degrees, for instance, the scan time would be just four and a half minutes. This can be easily computed with the rotating angular speed, resulting in 14,4 seconds to complete a revolution. Finally, the LIDAR device was simulated with a 40 Hz frequency of operation. Figure 4 displays the point cloud from the first example.

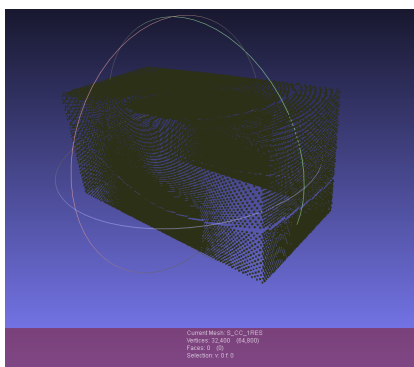


Fig. 4: Point cloud of a scanned cube. Visualized in MeshLab.

It is clear that even with the rotating pattern, the overall structure of the object appears intact. Figure 5 presents the digital reconstructed object.

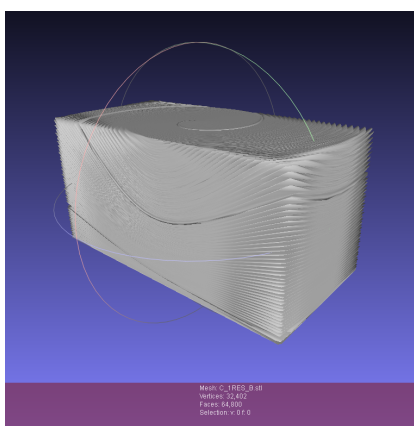


Fig. 5: Reconstructed STL from the point cloud from the first example. Visualized in MeshLab.

The sharp edges are produced by the way the points are scanned and reconstructed. There are two ways to address this and maintaining the reconstruction algorithm. One is by increasing the resolution, which will just mitigate the problem. The other is by applying a filter to the point cloud.

The length, width and height of the STL cube were measured in MeshLab and compared with the simulated and are described in Table I.

TABLE I: Measurement difference of the first example.

Length (%)	Width (%)	Height (%)
0.19	0.17	1.04

The dimensions of the first simulated object were  $0.2 \times 0.1 \times 0.1$  m (L x W x H). As can be seen from Table I, the differences are minimal.

A more complex object was scanned and reconstructed for the next example. It is composed of several regular polyhedrons and a sphere. This point cloud was already presented in Figure 2. The discontinuity between the sphere and the center cube can happen for three reasons. The angular speed of the rotating plate, the operation frequency of the LIDAR device and by the geometry of the object creating shades from the LIDAR point of view. Figure 6 displays the result of the reconstruction algorithm.

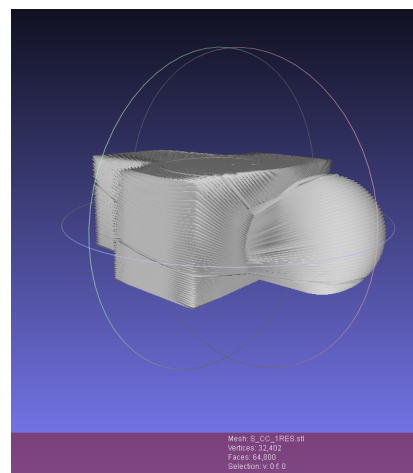


Fig. 6: Reconstructed STL from the point cloud from the second example. Visualized in MeshLab.

This example took roughly the same time to scan and generate the STL files.

The differences between the measurements and the actual simulated objects are described in Table II.

TABLE II: Measurement difference of the second example.

Object	Length (%)	Width (%)	Height (%)
Center cube	0.16	0.13	1.07
Side cube	1.02	1.06	0.97
Radius (%)			
Sphere	3.89		

The dimensions of the center cube are identical from example 1. The other two objects, namely the sphere and the side cube, have 0.05 m (R) and  $0.01 \times 0.01 \times 0.01$  m (L x W x H), respectively. As can be noted, the differences remain minimal.

Finally, a last example with a different arrangement of the polyhedrons and spheres is displayed in Figures 7 and 8.

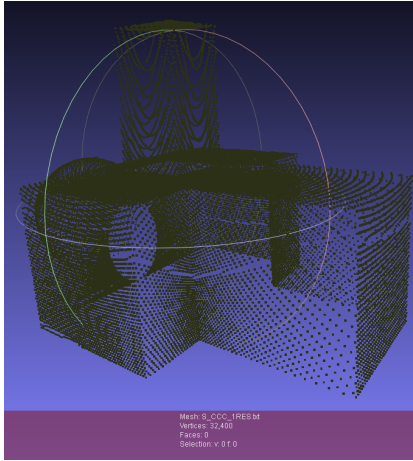


Fig. 7: Point cloud from the third example. Visualized in MeshLab.

The effects from the rotating platform are more evident the smaller the size of the object is. This can be clearly seen in the figure above, as the point lines in the top-most cube are more curved.

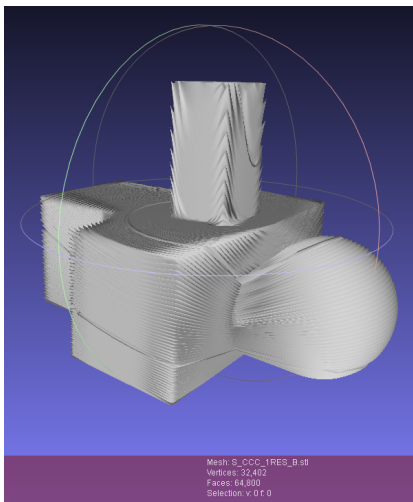


Fig. 8: Reconstructed STL from the point cloud from the third example. Visualized in MeshLab.

The time to scan the object and generate the STL files was the same as previous examples. The three examples had 64800 polygons and 32402 vertices. Finally, the point cloud and the generated STL can be seen overlapped in Figure 9.

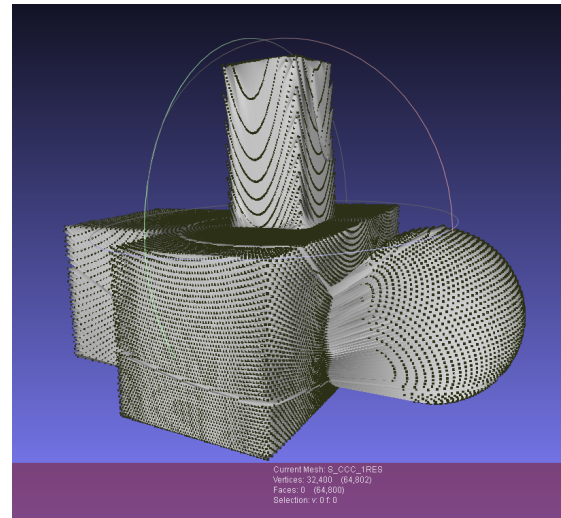


Fig. 9: Point cloud and generated STL overlapped. Visualized in MeshLab.

The overlap shows that the algorithm works as intended, even showing the behaviour from the rotating platform that creates the discontinuity from the line points between the sphere and the center cube.

The measurement differences of this example can be seen in Table III.

TABLE III: Measurement difference of the third example.

Object	Length (%)	Width (%)	Height (%)
Center cube	0.37	0.71	0.82
Side cube	1.41	1.27	0.34
Top cube	1.04	1.13	0.47
Radius (%)			
Sphere	1.72		

The only object with new dimensions is the top cube with  $0.05 \times 0.05 \times 0.1m$  (L x W x H). Same as previous examples, the differences remain minimal.

It is important to note that although errors were introduced during the point cloud acquisition, STL construction and the measuring phases, they did not affect in a significant way the percentage differences.

## V. CONCLUSION AND FUTURE WORK

This paper presented a simulated low-cost 3D scanning system that is composed of a LIDAR device, and an actuated platform and arc-shaped brace with stepper motors. The system is capable of scanning small objects with a great resolution and precision in a long, but acceptable time considering the system's limitations with a budget investment. The software algorithm is capable of reconstructing the point clouds generated by the scanning system with very fast speed with good resemblance of the original real-world objects. The proposed approach validates the algorithm and the mechanical solution that is being developed although with the delay of confinement. For future work, although a filter would smooth

out the sharp edges in the STL files, the reconstruction algorithm needs improvement. The tiny discontinuations between the scanning structure increments can be mitigated or outright removed with synchronization between the motors, stopping whenever the increment occurs. The discontinuations caused by the platform rotating speed needs to be improved. The prototype is in the progress of being constructed to be tested in a real scenario.

#### ACKNOWLEDGMENT

The project that gave rise to these results received the support of a fellowship from "la Caixa" Foundation (ID 100010434). The fellowship code is LCF/BQ/DI20/11780028. This work also has been supported by FCT – Fundação para a Ciência e Tecnologia within the Projects UIDB/50014/2020 and UIDB/05757/2020.

#### REFERENCES

- [1] Straub, J., & Kerlin, S. (2014). Development of a large, low-cost, instant 3D scanner. *Technologies*, 2(2), 76-95.
- [2] Straub, J., Kading, B., Mohammad, A., & Kerlin, S. (2015). Characterization of a large, low-cost 3D scanner. *Technologies*, 3(1), 19-36.
- [3] Rocchini, C. M. P. C., Cignoni, P., Montani, C., Pingi, P., & Scopigno, R. (2001, September). A low cost 3D scanner based on structured light. In *Computer Graphics Forum* (Vol. 20, No. 3, pp. 299-308). Oxford, UK and Boston, USA: Blackwell Publishers Ltd.
- [4] Bernardini, F., & Rushmeier, H. (2002, June). The 3D model acquisition pipeline. In *Computer graphics forum* (Vol. 21, No. 2, pp. 149-172). Oxford, UK: Blackwell Publishers Ltd.
- [5] Tong, J., Zhou, J., Liu, L., Pan, Z., & Yan, H. (2012). Scanning 3d full human bodies using kinects. *IEEE transactions on visualization and computer graphics*, 18(4), 643-650.
- [6] Levoy, M., Pulli, K., Curless, B., Rusinkiewicz, S., Koller, D., Pereira, L., ... & Shade, J. (2000, July). The digital Michelangelo project: 3D scanning of large statues. In *Proceedings of the 27th annual conference on Computer graphics and interactive techniques* (pp. 131-144).
- [7] Wulf, O., & Wagner, B. (2003, July). Fast 3D scanning methods for laser measurement systems. In *International conference on control systems and computer science (CSCS14)* (pp. 2-5).
- [8] Weise, T., Leibe, B., & Van Gool, L. (2007, June). Fast 3d scanning with automatic motion compensation. In *2007 IEEE Conference on Computer Vision and Pattern Recognition* (pp. 1-8). IEEE.
- [9] Remondino, F. (2011). Heritage recording and 3D modeling with photogrammetry and 3D scanning. *Remote sensing*, 3(6), 1104-1138.
- [10] Panjvani, K., Dinh, A. V., & Wahid, K. A. (2019). LiDARPheno—A Low-Cost LiDAR-Based 3D Scanning System for Leaf Morphological Trait Extraction. *Frontiers in plant science*, 10, 147.
- [11] Kimoto, K., Asada, N., Mori, T., Hara, Y., & Ohya, A. (2014, May). Development of small size 3D LIDAR. In *2014 IEEE International Conference on Robotics and Automation (ICRA)* (pp. 4620-4626). IEEE.
- [12] Dou, M., Taylor, J., Fuchs, H., Fitzgibbon, A., & Izadi, S. (2015). 3D scanning deformable objects with a single RGBD sensor. In *Proceedings of the IEEE Conference on Computer Vision and Pattern Recognition* (pp. 493-501).
- [13] Boehler, W., & Marbs, A. (2002). 3D scanning instruments. *Proceedings of the CIPA WG*, 6(9).
- [14] Costa, P., Gonçalves, J., Lima, J., & Malheiros, P. (2011). Simtwo realistic simulator: A tool for the development and validation of robot software. *Theory and Applications of Mathematics & Computer Science*, 1(1), 17-33.